Available online at www.sciencedirect.com
ScienceDirect
Journal of the European Ceramic Society 27 (2007) 2513–2519
www.elsevier.com/locate/jeurceramsoc

Investigation of residual stresses on the boundary of SiC/SiC + 20% TiB_2 composite materials joining by optic modulation–polarization method

L.I. Berezhinsky [a], I.L. Berezhinsky [b], O.N. Grigorev [b], B.K. Serdega [a,*], V.A. Ukhimchuk [a]

[a] *V.E. Lashkarev Institute of Semiconductor Physics, NASU, Kiev-28, Prospect Nauky, 41, Kyiv 03028, Ukraine*
[b] *I.M. Frantsevich Institute for Problem of Material Sciences, NASU, Kiev-142, str. Krzhizhanovsky, 3, Kyiv 03142, Ukraine*

Received 1 June 2006; received in revised form 14 August 2006; accepted 18 August 2006
Available online 2 October 2006

Abstract

The optical method of registration of internal stresses in composite materials is offered. The method is based on the modulation of polarization of laser radiation reflected from anisotropic media and the definition of its anisotropy parameters by means of this modulation. Residual stresses on the border of SiC/SiC + 20% TiB_2 joining, caused by the difference of temperature expansion coefficients, were studied by the offered method. The experimental curve of stress distribution is in a good qualitative agreement with theoretical calculation. The stress magnitude obtained by the given method well coincides with the values obtained by a Raman scattering method and diffraction of X-ray radiation.

PACS: 81.05.Mh; 07.10.Lw

Keywords: Joining; Composites; Strength; Stress; SiC

1. Introduction

Distribution of the residual stresses on the border of two joined composite materials caused by the difference of their thermal expansion coefficients is a very important characteristic determining mechanical properties of this connection. Such information is especially important for the development of multilayer composite materials.

The recently developed layered composite materials representing alternate layers of composite ceramics (thickness of some tens microns) and metal or other plastic materials (thickness of a few microns) are the most perspective for creation of light-weight and ultra-strong materials. In comparison with a solid mass of cermet, they have the best mechanical characteristics; in particular they stand the higher stresses, which correspond to a critical level of elastic deformation, and also have higher ability to resist the impact load. If we take into account that such materials stand a high temperature and pressure and are capable of working in aggressive environments, there are no doubts that such materials are extremely required in aircraft, space, rocket, atom-energy engineering. The offered optical method of definition of internal stresses in composite materials is intended first of all for development of such materials. It is explained by the fact that knowledge about stresses inside layers and especially stress distribution on the border between layers is the most valuable information for modeling, accounts and creation of the appropriate materials. The use of X-ray methods for obtaining such information in this case is unpromising because the intensity of X-ray beams with a diameter of about 10 μm of real X-ray sources is very small, except for a synchrotron source.

2. Experiment and samples

2.1. Physical principle of a method and optical schema of a setup

The photo elastic effect is widely used in engineering for the control of stresses in various mechanical details. However, this effect can be observed only on transparent materials. This circumstance limits the opportunities of this method because it is needed to make the simulated copies of researched objects

* Corresponding author. Tel.: +380 44 525 5778.
E-mail addresses: oleggrig@ipms.kiev.ua (O.N. Grigorev), serdega@isp.kiev.ua (B.K. Serdega).

0955-2219/$ – see front matter © 2006 Elsevier Ltd. All rights reserved.
doi:10.1016/j.jeurceramsoc.2006.08.017

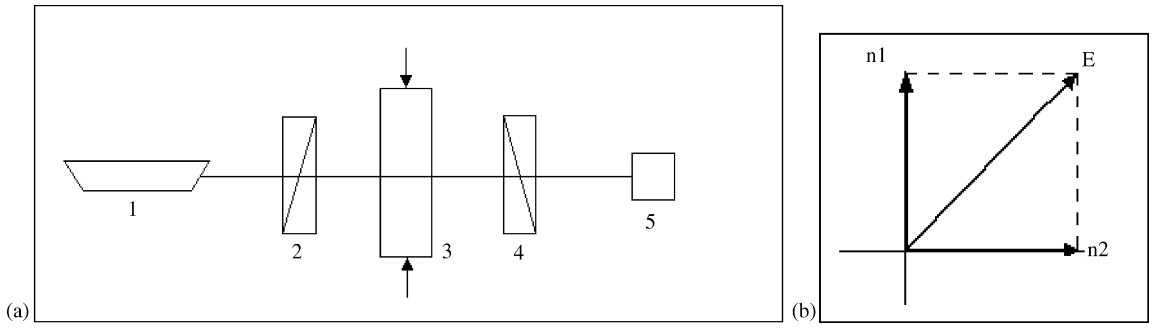

Fig. 1. The optical schema for supervision of photoelastic effect: (a) 1, laser; 2 and 4, polarizers; 3, sample; 5, photo diode; arrows specify external pressure and (b) orientation of an electric field of a light wave concerning anisotropic axes.

of a glass, plastic or other transparent materials. The offered method is suitable for researches on both transparent and opaque materials, since it can operate in transmittance and reflection mode.

Let the light from a source after passing through a polarizer falls normally on a sample to which the external pressure is applied (Fig. 1a). Let us assume that the polarization plane of the polarizer makes an angle of 45° with the direction of the applied pressure. Then the propagation process of a light wave with such a polarization through a sample can be considered as a propagation of two waves with mutually orthogonal polarizations (Fig. 1b). However, as the refractive index for a wave polarized vertically is more (because a sample in this direction is compressed), the propagation velocity of this wave will be less than that for a light wave polarized horizontally (sample in this direction is stretched). The phase difference between waves will be observed at the exit of a sample

$$\varphi = \frac{2\pi}{\lambda} L \Delta n, \tag{1}$$

here λ is the wavelength of light, and L is sample thickness

$$\Delta n = n_1 - n_2 = \Pi(\sigma_1 - \sigma_2), \tag{2}$$

here Π is tensor of elastooptic coefficients, and n_1, n_2, σ_1, σ_2 are refractive indexes and stresses along respective directions. Thus, it is visible from the formulas (1) and (2) that the phase difference is directly proportional to stress value $(\sigma_1 - \sigma_2)$.

Linearly polarized light, falling on the sample, changes the polarization depending on a φ value. So, at $\varphi = \pi/2$, linearly polarized light will be transformed to circularly polarized, and at $\varphi = \pi$, it will be transformed to orthogonally polarized. In all other cases (when $\varphi \neq \pi/2$ or π), linearly polarized light will be transformed to elliptically polarized light. Thus, the intensity of circularly polarized component in elliptically polarized radiation is proportional to $(\sigma_1 - \sigma_2)$ value.

The optical schema of setup is shown in Fig. 2. Its operation principle consists of the following: the laser radiation ($\lambda = 0.63$ or 1.15 μm), polarized at angle of 45° to *X*- and *Y*- axes, is directed on the splitter and is split into two equal intensity beams. One of them is directed on the anisotropic reflector R (quarter wave plate) and another on a sample S. After reflection, both beams are reunited and through the polarizing modulator PM and polarizer P are directed on the photo diode PD. When the schema operates in "transmission" mode, the mirror is put after the sample.

If the polarization planes of the polarizer P and laser radiation are crossed, the photo diode does not show any signal. However, imperfections of optical elements of the schema can cause some signal on the photo diode. Turning the reflector R around an axis, this detector signal can be compensated. Initial condition of polarization state is thus established. If now a sample is moved in other place, where there is internal stress, or it is created artificially, the radiation reflected from a sample will not be already linearly polarized (as falling radiation) and will have elliptic polarization. The elliptic polarization is a mix of linearly and circularly polarized light. As it was stated above, the intensity of a circular component is proportional to the magnitude of stress $(\sigma_1 - \sigma_2)$. The polarization modulator (PM)[1] is a special device that allows to register intensity only the circular (or linear) components of the elliptically polarized light. Thus, by scanning the sample surface by a laser beam and registering the intensity of circularly polarized light, it is possible to register the stress distribution along the scan in real time.

The spatial resolution of setup is defined by a diameter of a laser beam, which falls on a sample. Therefore, to increase the spatial resolution, the micro-objective O1 is placed before the

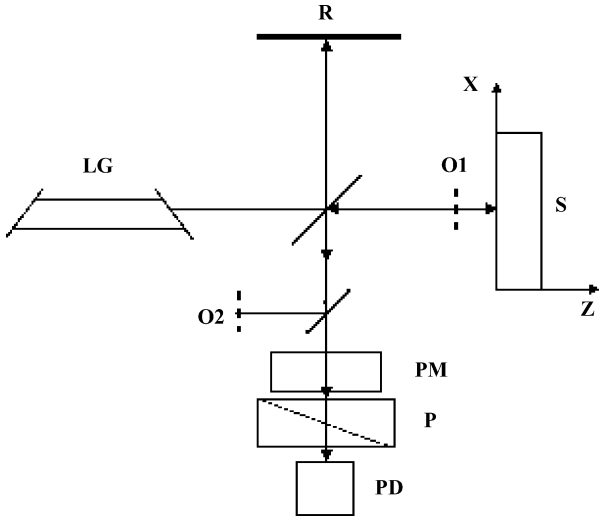

Fig. 2. The optical schema of setup for supervision of internal stresses in opaque materials: LG, He–Ne laser; R, λ/4 plate; PM, polarizing modulator; P, polarizer; PD, photo diode; O1, micro-objective; O2, eyepiece.

sample. Micro-objective allows to focus a laser radiation on a sample in the spot by a diameter of a several micrometers. The supervision of a spot size and its location on a sample surface is carried out through the eyepiece O2. Micro-objective O1 and eyepiece O2 are installed in such a manner that together they form a microscope.

The setup allows to register a signal proportional to the value of $(\sigma_1 - \sigma_2)$, which is recorded by a plotter in relative units. However, stress distribution can be submitted in absolute units. In this case, the setup should be calibrated.

2.2. Samples

Samples of two-layer ceramics SiC/SiC + 20% TiB_2 were made as follows. The briquettes (tablets) of SiC and SiC + 20% TiB_2 with a diameter of ∼10 mm and thickness of 5 mm were made of 5–10 μm powders of SiC (mark a-SiCM5 of Zaporozhye abrasive factory) and TiB_2 (mark THAT 6-09-03-7-75 of Donetsk chemical factory). The briquettes were made at a pressure of 30 MPa. Then the briquettes, one after another, were consistently put in the graphite mold and were exposed to hot pressing in the industrial induction furnace (SPD-120) without shielding medium. The parameters of isothermal annealing were as follows: duration 15–20 min, temperature 2000–2100 °C and pressure 30 MPa. The speed of heating up to annealing temperature was 100 °C min^{-1}. Upon termination of isothermal annealing ceramics cooled in the mold under pressure together with installation up to a temperature of 1100 °C with a speed ∼100 °C min^{-1}. At the temperature of 1100 °C, the pressure was removed and mold was located in the heat-insulated chamber, in which it slowly cooled down to room temperature in a natural way.

Samples of the size of 3 mm × 3 mm × 8 mm were cut out from the obtained ceramic cylinder along its axis. Sawing was carried out by a diamond wheel with the grain size of 100 μm. Then the samples were ground and polished with diamond paste with a grain of 1 μm in the last stage of polishing.

The slip molding method of thin films was used in the making of multi-layer samples. The 50 μm thickness film was fabricated on the injection-molding machine of various powders mixed with components on the rubber basis. To exclude molding defects, the film was folded in a roll and then rolled up to a thickness of 150–200 μm. The samples of the necessary size were cut out from the obtained SiC and TiB_2 sheets, and a package of 11–13 alternating layers was made. Then the package was sintered according to the same technological parameters.

3. Results

3.1. Experimental function of stress distribution

The results of scanning of the contact region of a SiC composite ceramic and SiC + 20% TiB_2 composite by a laser beam with a 25 μm diameter are submitted in Fig. 3. On the abscissa axis, the coordinate is pointed and magnitude of signal at every point of scan is pointed on the of ordinate axis. As magnitude of signal is proportional to stress value $(\sigma_1 - \sigma_2)$, we can believe

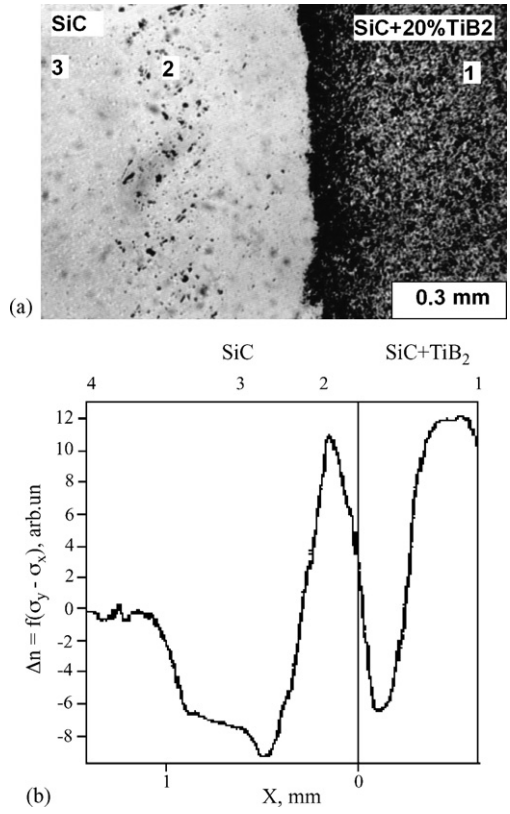

Fig. 3. The surface morphology of double-layer ceramic (a) and the curve of its scan by laser beam (b). The zones of registration of Raman spectra are numbered as 1–4.

that function $\Delta n = f(\sigma_y - \sigma_x)$ describes the stresses distribution. It is visible that to the left of conditional border (deep into SiC), the stress grows and achieves a maximum at a distance of 0.3 mm from the border. Then the stresses decreases, changes the sign, achieves minimum and then grows to a zero level.

The pores have been revealed in the region of large stresses (zone 2 in Fig. 3) by the observation of sample surface in metallurgical microscope. It is necessary to note that pores are an additional source of internal stresses in a composite material. It is well demonstrated in Fig. 4, where the stress distribution of multi-layer composite sample is shown. This sample contained 13 alternating layers of SiC and TiB_2. The thickness of SiC layers was made 220–240 μm and that of TiB_2 approximately 300 μm. The morphology of a sample surface is shown in Fig. 4a where pores are visible in a TiB_2 layer. The stress distribution of a sample part containing two TiB_2 layers and two SiC layers is shown in Fig. 4b. The spot of a probe laser beam on the sample surface was made 25 μm, which had allowed to define a local heterogeneity of stress distribution inside TiB_2 layers.

As the information about stresses is obtained by measuring the intensity of circularly polarized components of the light reflected from a sample, the presence of defects on its surface can distort the obtained information. For example, the scattering on the surface defects change intensity of the reflected laser beam, and consequently the intensity of circularly polarized component too. Therefore, to exclude influence of surface defects on the obtained results, the measurements were carried out as fol-

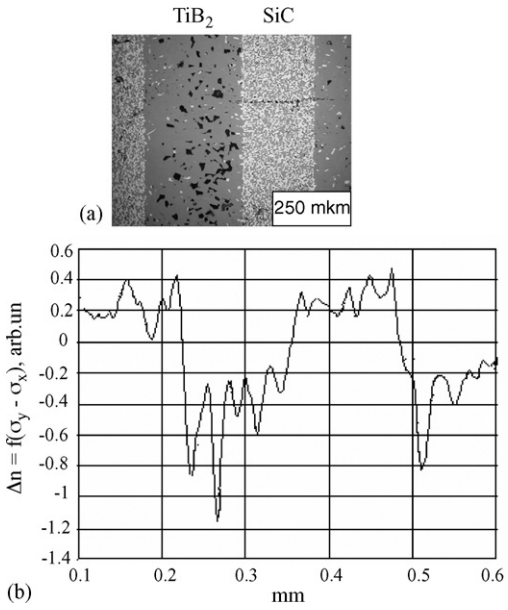

Fig. 4. The surface morphology of multi-layer SiC/TiB_2 composite (a) and distribution of its internal stresses in a direction normal to the plane of layers.

lows: the scan of stress distribution was recorded two to three times, to be sure that the scanning was made on the same line. Then the laser beam was modulated by a mechanical disk chopper with a certain frequency. At this frequency, the intensity of reflected light was registered by a method of synchronous detecting at the scanning of sample along the same line. Then the errors caused by surface defects were eliminated by a division of one signal on another.

Let us note that the heterogeneities of stress distribution found out within each layer are caused by high sensitivity of a method to defective structure of layers.

3.2. Research of the strain–stress states by a Raman scattering method

The strain–stress state of SiC composite ceramics in various points near the border of SiC/SiC + 20% TiB_2 composites was investigated by the Raman scattering method. The spectra were registered by means of a DFS-24 (LOMO USSR) spectrometer in a photon account mode. Ar-laser ($\lambda = 5145$ Å) with a power of about 100 mW in a line was used for excitation of Raman spectra. Spectral width of an entrance slit of spectrometer was made 1 cm^{-1} that provided enough high resolution. The repeatability of spectra had size not less than 1 cm^{-1} on the frequency scale. The spectra were registered from various zones of a sample surface (see Fig. 3). For this purpose, the laser beam was focused at a spot of 100 μm in diameter. Since sample was manufactured from SiC and TiB_2 powders of 5–10 μm size, it is possible to think that at such a size of a laser spot, the general Raman spectra always had been obtain. In other words, the registered spectra always contained all bands of SiC lattice vibrations allowable by a selection rule for various polarizations because a lot of microcrystals with random orientations are contained on the area of laser spot.

The Raman spectra were registered in the region of TO vibrations since in this region, distinctions in vibration frequencies of various SiC polytypes are observed. The Raman spectra observable in various zones of a sample are shown in Fig. 5. In zone 1, representing a composite SiC + 20% TiB_2, the bands with frequencies 769, 790 and 796 cm^{-1} are observed (curve 1), which correspond to 6H SiC polytype.[2] The wide band with small intensity at 745 cm^{-1} probably belongs to TiB_2. High general background of this spectrum was caused by a contribution of a Rayleigh scattering band. Such its large extent is caused by a significant optical heterogeneity of composite material SiC + 20% TiB_2.

The wide band representing a set of overlapped bands is observed in zones 2, 3 and 4. Therefore, in every case for determination of vibration frequencies in the maximums of a corresponding bands, the computer decomposition on the components of a wide band contour was carried out.

Bands with maximums 778, 789 and 797 cm^{-1} are observed in Raman spectrum obtained from zone 2 (curve 2). The frequencies 778 and 789 cm^{-1} are in a good accordance with vibration frequencies as 776 and 787 cm^{-1} of 4H SiC polytype.[3] And what is more, a relative intensity of these bands also is in complete accordance with data of work.[3] However, observable shoulder 797 cm^{-1} is not characteristic for 4H SiC polytype. Frequency of this peak corresponds to a 6H SiC polytype, however relative intensity of this band is much higher, than it is observed in 6H SiC spectrum (curve 1). Besides, if this band indeed belongs to 6H SiC polytype, than in this case the peak of 790 cm^{-1} should be observed because its intensity on the order is higher than peak 796 cm^{-1}. Therefore, it is more preferable to believe, that the peak 797 cm^{-1} on a curve 2 belongs to 3C SiC polytype.

The Raman spectrum of 3C SiC polytype was investigated by the authors of work.[4] Raman spectra of 3C and 6H SiC polytypes were compared in this work. It was shown that in area TO vibrations both polytypes have a band with frequency 796 cm^{-1}, however in 3C SiC the intensity of this peak is higher on the order, than in 6H. Since in this spectrum (curve 2) other bands, except band of 797 cm^{-1}, characteristic for 6H are not observed, so with the greater probability it can be identified as band of TO vibration of 3C SiC polytype.

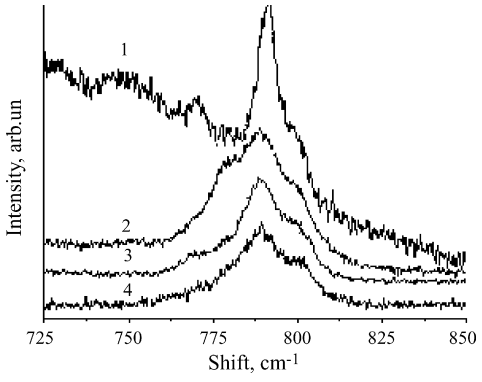

Fig. 5. Raman spectra from various zones accordingly with designations in Fig. 3.

Raman spectrum of area 3 is shown in Fig. 5, curve 3. Peaks 767, 788 and 794 cm^{-1} are observed here. Qualitatively spectrum well corresponds to 6H SiC spectrum (curve 1), however frequencies are moved approximately on 2 cm^{-1} to small energy. Moreover, the bands in spectrum 3 are wider than in spectrum 1. In addition, the band of 794 cm^{-1} has a large relative intensity that is not peculiar for 6H SiC polytype. If to assume that the peak 788 cm^{-1} belongs to 4H SiC polytype, it is impossible to explain absence other band 776 cm^{-1} peculiar to this polytype, which intensity is comparable with peak 788 cm^{-1}. It is more probable to assume that this spectrum (curve 3) belongs to 6H SiC polytype, bands of which are moved on 2 cm^{-1} to small energy. The presence of 3C SiC polytype allows to explain the enough high relative intensity of 794 cm^{-1} band.

The peaks 769, 790 and 796 cm^{-1} corresponding to 6H SiC (as a curve 1) are observed in Raman spectrum obtained in area on a distance of 3–4 mm from conditional border (curve 4, Fig. 5). The large width of 790 cm^{-1} peak and high intensity of peak 796 cm^{-1} can be explained by presence of 4H and 3C SiC polytypes.

4. Discussion

The observed Raman spectra find a satisfactory explanation, if to take into account technology of manufacturing of samples. Samples were produced from commercial 6H SiC powders of Zaporozhye abrasive factory. The share of 4H and 3C polytypes in this powder consists of about 1–2%. The samples have been manufactured by a sintering method of the briquettes and have been under pressure of 30 MPa at temperature 2100 °C during 15 min. Then they have been cooled to room temperature. Such thermal treatment can result in phase transformations of SiC. Really, Si–C state[5] shows, that there is a balance between a liquid and crystal phases of SiC at a pressure of 10 MPa and temperature more than 1410 °C. The cooling up to temperature 1000–1100 °C occurs at an external pressure of 30 MPa therefore, the growth of 4H and 3C SiC grains is quite possible at presence of proper inoculating crystals. The 4H SiC grains are usually found out as columnar crystals under microscope in hot-pressured ceramics. The self-reinforcement effect in structures on basis of α-SiC occurs because of a high anisotropy of the grain sizes of this polytype.

The thermodynamic consideration of process of SiC phase transitions shows that the most stable are the polytypes, whose entropy is more.[6] It means that the most stable polytypes formed in our conditions, can be 2H, 4H and 3C. It is proved by the experiment: recrystallization of 6H polytype in 4H and 3C is observed at an increase of SiC vapor pressure or concentration of impurity nitrogen atoms.[6]

If to take into account the above mentioned details, 778 and 789 cm^{-1} bands observed in a Raman spectrum (Fig. 5, curve 2) can be attributed to a polytype 4H SiC, and 797 cm^{-1} band to a polytype 3C. However, observable frequencies 4H and 3C on 1–2 cm^{-1} are moved to large energy in comparison with the data.[3,4] It is possible to explain such shift by internal stress in this area of a sample, which is fixed experimentally (Fig. 3b). The absolute value of this stress consists about 0.2 GPa and it was obtained by means of standard curve of installation.

Frequency shift of TO phonons in SiC crystal at hydrostatic pressure consists 3.5 ± 0.2 cm^{-1} GPa^{-1}.[7] Taking this result into account, it is possible to expect a shift of TO phonon frequency approximately on 1 cm^{-1} at pressure 0.25 GPa (magnitude of stress registered experimentally in the area 2, Fig. 5). The frequency shift on 1–2 cm^{-1} observable by us in Raman spectrum (Fig. 5, curve 2) can be caused by stress state of 4H and 3C SiC, because in our case the pressure is not hydrostatic.

Bands of 767, 788 and 794 cm^{-1} on curve 3 in Fig. 5 may be attributed to 6H SiC polytype, which is in the stretched state because frequencies of its TO phonons are moved on 2 cm^{-1} in the smaller energy in comparison with frequencies observed on curve 1. It is confirmed by curve form of stress distribution (Fig. 3b), from which it is visible, that after a zone of compression 2 the zone of a stretching 3 follows. At that the numerical values of observable stresses in these zones are almost equal.

General form of stress distribution curve (Fig. 3b) allows to explain the cause of appearance of pores in area 2. Diamond powder during a mechanical polishing of a composite sample had picked out the micro-crystals in the stress state.

The form of curve of observed stress distribution (Fig. 3b) is in the good agreement with results of work.[8] Authors of this work investigated the residual stresses on a connection border of ceramics Al_2O_3 with a composite 60% Al_2O_3 + 40% Ni. It was shown that the maximal compression of Al_2O_3 ceramics caused by distinction of temperature expansion coefficients is on a distance of 0.5 mm from conditional border of the unit. In our case, this distance is 0.25–0.3 mm that is in the good agreement. It is necessary to note, that a difference of temperature expansion coefficients of joint materials in work[8] much more than in our case. Because the authors of the mentioned work used samples of the cylindrical form (diameter of 8 mm and length of 23 mm), therefore distribution of stresses had an axial symmetry. In our case, samples had the parallelepiped form, therefore symmetry of distribution of stresses was other.

However, it is necessary to note that the experimentally observed distribution of stresses in our case (Fig. 3b) very well agrees qualitatively with theoretical curve calculated by the authors of work[8] by a final elements method.

Distinctive feature of offered polarization–modulation method is the fact, that it gives the stress distribution as function $(\sigma_y - \sigma_x)$, where x (in our case) is directed perpendicular to plane of joining. This method does not allows to obtain distribution $(\sigma_y + \sigma_x)$ by any optical measurements with the purpose of definition σ_y and σ_x separately. However, the fact that a maximum $(\sigma_y - \sigma_x)$ is in a point removed from border of the unit on some distance, testifies the presence of significant stresses directed on normal to border.

Let us make estimations of stress magnitude, which can arise on border SiC/SiC + 20% TiB_2 as a result of difference of temperature expansion coefficients. The temperature expansion coefficients and Young modulus in the temperature interval 0–1000 °C for SiC and TiB_2 are equal accordingly[9]: $\alpha_{SiC} = 5.68 \times 10^{-6}\ K^{-1}$, $E_{SiC} = 500$ GPa, $\alpha_{TiB_2} = 8.1 \times 10^{-6}\ K^{-1}$, $E_{TiB_2} = 660$ GPa. We can calculate the corresponding param-

eters for a composite material SiC + 20% TiB_2 by using the following formula[10]

$$\alpha_{comp} = \alpha_{SiC} V_{SiC} + \alpha_{TiB_2} V_{TiB_2},$$
$$E_{comp} = E_{SiC} V_{SiC} + E_{TiB_2} V_{TiB_2},$$

where V_{SiC} and V_{TiB_2} are volume fractions of a component forming a composite material.

However, to make estimations of stresses under the following formula which is taking into account thermal and elastic deformations

$$\sigma = E(\varepsilon + \alpha \Delta T)$$

is impossible, because the strain ε are unknown. Nevertheless, the estimation of stress arising in ceramics SiC under action of compressing effort of a composite SiC + 20% TiB_2 at the account only of temperature deformations gives magnitude 0.25–0.3 GPa. The order of this value is in good conformity with experimentally observable stress of 0.2 GPa. It is necessary to note that experimentally obtained stress value of 0.2 GPa from Raman spectra well agree with data in work.[11] In this work by an X-ray method it is established that in a composite material SiC + 20% TiB_2, the SiC grains test a compressing pressure of 250 MPa.

It is necessary to note that the stress component normal to interface of two media is defined as not only difference of temperature expansion coefficient, but also technological process and its parameters (temperature range of cooling). So physical properties of materials such as mutual adhesion, diffusion, wetting, etc., will have influence on mechanical strength of a joining. For example, SiC/SiC + 10% TiB_2 border prepared in the same conditions as SiC/SiC + 20% TiB_2 a stress zone in SiC, similar 2 in Fig. 3, is not observed. At the same time, the increase of concentration TiB_2 up to 30% results that the SiC/SiC + 30% TiB_2 border is flaked off. Nevertheless, multi-layer composite material containing 15 alternate layers of SiC and TiB_2 was obtained by means of perfection of technology.

Fig. 4 shows a distribution of stresses on the borders of SiC and TiB_2 layers in this composite material. It was established that SiC layers are compressed and TiB_2 layers are stretched. There are cracks in SiC layer directed along normal to contact plane of materials. The local heterogeneities of stress distribution are observed in TiB_2 layer, which are caused of appearance of pores at machining treatment.

The form of curve, showing a stress distribution on the contact border of two composite materials with various temperature expansion coefficients, may be explained being based on a general reasons. As a rule contacting composite materials cool down from temperature T to T_{room}. The strain size of each of them consists of lengthening caused by change of temperature and by stress. According to the general thermoelasticity theory, this strain is bound up with stress and elastic constants of substance by the following ratio[12]:

$$\varepsilon_{ik} = \frac{1}{2G}\left[\sigma_{ik} - \frac{\mu}{1+\mu} s\delta_{ik}\right] + \alpha T \delta_{ik},$$

where ε_{ik} and σ_{ik} are components of strain and stress tensor, respectively, μ the Poison constant and s is sum of normal stresses

$$s = \sigma_{xx} + \sigma_{yy} + \sigma_{zz},$$

α is temperature expansion coefficients, δ_{ik} the Kronnecker symbol ($\delta = 0$ if $i \neq k$, и $\delta = 1$ if $i = k$) and G is modulus of rigidity, bound up with modulus of elasticity E (Young) by relationship

$$2G = \frac{E}{1+\mu}$$

In the monograph[12] it is shown that according to thermoelasticity theory

$$\varepsilon_{ik} = \frac{\partial^2 \Phi}{\partial i \partial k}, \qquad \sigma_{ik} = 2G\left[\frac{\partial^2 \Phi}{\partial i \partial k} - \Delta\Phi\delta_{ik}\right], \tag{3}$$

where Φ is a function named as thermoelastic potential of displacement and can be determined from the Poisson equation

$$\Delta\Phi = \frac{1+\mu}{1-\mu}\alpha T,$$

where T is a function of coordinates and time. To decide this equation in partial derivative, it is necessary to know spatial boundary conditions and conditions at the moment of time $t = 0$. The spatial boundary conditions stipulate the influence of environment on a surface temperature of a body. In general case, the environment temperature and law of heat exchange between a surface and external medium is given. To obtain a general decision of this task are very difficult. Therefore, as a rule the partial solution is found and then the satisfactions of boundary conditions is required. Function Φ easier all is defined for a stationary case, i.e. when the distribution of temperature does not change in time. In a non-stationary case the calculation is considerably complicated.

Let us assume that we are able to calculate function Φ. In spite of the fact that both contacting materials are in identical conditions, functions Φ_1 and Φ_2 will be different because elastic properties of materials are different. In other words, in the graph $\Phi(x)$ the values of functions Φ_1 and Φ_2 are different on the different sides from conditional border of two materials. We can represent them as two different levels (Fig. 6a). In transition region these functions should smoothly pass one in another (Fig. 6a), because we have smooth transition from one material to another.

According to Eq. (3), a stress distributions on the border of two materials is second derivative from function Φ, i.e. the curve 3 in Fig. 6. The form of this curve is in good conformity with a theoretical curve calculated in work[8] and in good agreement with our experimental results.

Diffusion of atoms of one material into another takes place at a high temperature, and this should result in stress distribution on the border. Therefore, real distribution of internal stresses near the border of two materials represents total distribution as thermoelastic stresses and internal stresses of other nature therefore, the form of a curve (Fig. 6, curve 3) would be deformed.

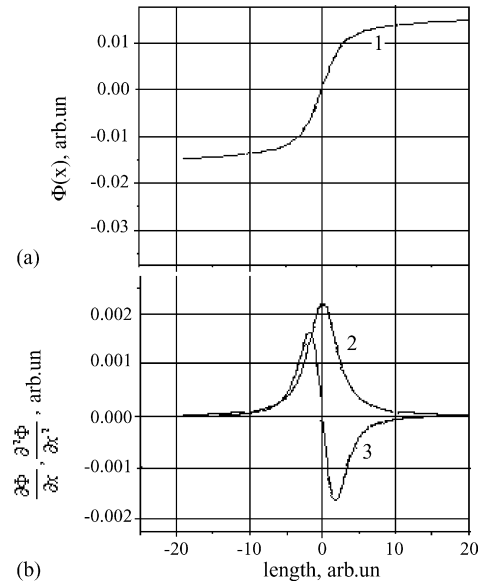

Fig. 6. The conditional image of $\Phi(x)$ function on the connection border of two composite materials (1) and diagrams of its first (2) and second (3) derivatives.

5. Conclusions

1. The offered modulation–polarization method of registration of internal stresses in composite materials is very informative and easily realizable in any research laboratory.
2. The method allows not only to obtain real curves of stress distribution in composite materials, but also to estimate their absolute values.
3. Concerning multi-layer composite materials, the offered method today is the single simple and accessible method for experimental registration of stress distribution on the borders of layers because use of X-ray methods in this case is difficult and ineffective.
4. The modulation–polarization method of definition of internal stresses is much easier, and is more cheaply, more safely and technically more easily realizable than the methods based on neutrons diffraction or synchroton radiation.
5. The use of the offered method for investigation of residual stresses on the border of two joined composite materials has shown the following:
   - curve of stress distribution has an S-form concerning conditional border and corresponds qualitatively well to a theoretical curve calculated by a final element method,[8]
   - experimentally obtained numerical values of stresses have a good agreement both with numerical estimations and with numerical values obtained from Raman spectra.

References

1. Jasperson, S. N. and Sahnatterly, S. E., An improved method for high reflectivity ellipsometry based on a new polarization modulation technique. *Rev. Sci. Instrum.*, 1969, **40**(6), 761–767.
2. Feldman, D. W., Parker James Jr., H., Choyke, W. J. and Patric, L., Raman scattering in 6H SiC. *Phys. Rev.*, 1968, **170**, 698.
3. Feldman, D. W., Parker James Jr, H., Choyke, W. J. and Patric, L., Phonon dispersion curves by Raman scattering SiC politypes 3C, 4H, 6H, 15R and 21R. *Phys. Rev.*, 1968, **173**, 787–793.
4. Okumura, H., Sakuma, E., Lee, J. H., Mukaida, H., Misawa, S., Endo, K. and Yoshida, S., Raman scattering of SiC: application to identification of heteroepitaxy of SiC polytypes. *J. Appl. Phys.*, 1987, **61**(3), 1134–1136.
5. Knippenberg, W. F. and Verspni, G., The influence of impurities on the growth of silicon carbide crystals by recrystalization. In *Silicon Carbide*, ed. H. K. Henisch and R. Roy. Pergamon Press, 1966, pp. 45–56.
6. Gnesin, G. G., *Silicon Carbide Materials*. Metallurgy, 1977, 214 pp. (in Russian).
7. Gregorio, J. F. and Furtak, T. E., Analysis of residual stress in 6H-SiC particles with Al_2O_3/SiC composites through Raman spectroscopy. *J. Am. Ceram. Soc.*, 1992, **75**(5), 1854–1857.
8. Rabin Barry, H., Williamson Richard, L. and Bruck Hugh, A., Residual strains in an Al_2O_3–Ni joint bonded with a composite interlayer: experimental measurements and FEM analyses. *J. Am. Ceram. Soc.*, 1998, **81**(6), 1541–1549.
9. Andrievsky, R. A. and Spivak, I. I., *Strength of Refractory Compounds and Materials on its Base*. Metallurgy Publishers, Chelyabinsk, 1989, 389 pp. (in Russian).
10. Tamura, I., Tomota, Y. and Ozawa, H., In *Proceedings of Third International Conference on Strength of Materials and Alloys*, 1973, p. 611.
11. Grigorev, O. N., Kovalchuk, V. V. and Subbotin, V. I., The structure and properties of SiC–MEB_2 ceramic. *J. Mater. Process. Manuf. Sci.*, 1998, **7**(1), 99–110.
12. Melan, E. and Parkus, H., *Wärmespannungen Infolge Stationärer Temperaturfelder*. Springer-Verlag, Wien, 1953.